

Manuscript Number: ATMOSRES-D-16-00177R2

Title: Hourly composition of gas and particle phase pollutants at a central urban background site in Milan, Italy

Article Type: Research Paper

Section/Category: aerosol particles

Keywords: PM2.5; hourly ionic composition; gas-phase pollutants; Po valley

Corresponding Author: Dr. Andrea Piazzalunga,

Corresponding Author's Institution:

First Author: Alessandro Bigi

Order of Authors: Alessandro Bigi; Federico Bianchi; Gianluigi De Gennaro; Alessia Di Gilio; Paola Fermo; Grazia Ghermandi; André Prévôt; Monia Urbani; Gianluigi Valli; Roberta Vecchi; Andrea Piazzalunga

Abstract: A comprehensive range of gas and particle phase pollutants were sampled at 1-hour time resolution in urban background Milan during summer 2012. Measurements include several soluble inorganic aerosols (Cl<sup>-</sup>, NO<sub>2</sub><sup>-</sup>, NO<sub>3</sub><sup>-</sup>, SO<sub>4</sub><sup>2-</sup>, Ca<sup>++</sup>, K<sup>+</sup>, Mg<sup>++</sup>, Na<sup>+</sup>, NH<sub>4</sub><sup>+</sup>) and gases (HCl, HNO<sub>2</sub>, HNO<sub>3</sub>, NH<sub>3</sub>, NO, NO<sub>2</sub>, O<sub>3</sub>, SO<sub>2</sub>), organic, elemental and black carbon and meteorological parameters. Analysis methods used include mean diurnal pattern on weekdays and Sundays, pollution roses, bivariate polar plots and statistical models using backtrajectories. Results show how nitrous acid (HONO) was mainly formed heterogeneously at nighttime, with a dependence of its formation rate on NO<sub>2</sub> consistent with observations during the last HONO campaign in Milan in summer 1998, although since 1998 a drop in HONO levels occurred following to the decrease of its precursors. Nitrate showed two main formation mechanisms: one occurring through N<sub>2</sub>O<sub>5</sub> at nighttime and leading to nitrate formation onto existing particles; another occurring both daytime and nighttime following the homogeneous reaction of ammonia gas with nitric acid gas. Air masses reaching Milan influenced nitrate formation depending on their content in ammonia and the timing of arrival. Notwithstanding the low level of SO<sub>2</sub> in Milan, its peaks were associated to point source emissions in the Po valley or shipping and power plant emissions SW of Milan, beyond the Apennines. A distinctive pattern for HCl was observed, featured by an afternoon peak and a morning minimum, and best correlated to atmospheric temperature, although it was not possible to identify any specific source. The ratio of primary-dominated organic carbon and elemental carbon on hourly PM<sub>2.5</sub> resulted 1.7. Black carbon was highly correlated to elemental carbon and the average mass absorption coefficient resulted MAC = 13.8±0.2 m<sup>2</sup>g<sup>-1</sup>. It is noteworthy how air quality for a large metropolitan area, in a confined valley and under enduring atmospheric stability, is nonetheless influenced by sources within and outside the valley.

# Hourly composition of gas and particle phase pollutants at a central urban background site in Milan, Italy

A. Bigi<sup>a</sup>, F. Bianchi<sup>b,c</sup>, G. De Gennaro<sup>d</sup>, A. Di Gilio<sup>d,h</sup>, P. Fermo<sup>e</sup>,  
G. Ghermandi<sup>a</sup>, A. S. H. Prévôt<sup>b</sup>, M. Urbani<sup>e,i</sup>, G. Valli<sup>f</sup>, R. Vecchi<sup>f</sup>,  
A. Piazzalunga<sup>g,j</sup>

<sup>a</sup>*Department of Engineering “Enzo Ferrari”, Università degli studi di Modena e Reggio Emilia, Modena, Italy*

<sup>b</sup>*Laboratory of Atmospheric Chemistry, Paul Scherrer Institute, Villigen, Switzerland*

<sup>c</sup>*Department of Physics, University of Helsinki, Helsinki, Finland*

<sup>d</sup>*Department of Chemistry, Università degli studi di Bari, Bari, Italy*

<sup>e</sup>*Department of Chemistry, Università degli studi di Milano, Milan, Italy*

<sup>f</sup>*Department of Physics, Università degli studi di Milano, Milan, Italy*

<sup>g</sup>*Department of Environmental Sciences, Università degli studi di Milano Bicocca, Milan, Italy*

<sup>h</sup>*Now at ARPA Puglia, Bari, Italy*

<sup>i</sup>*Now at Chemservice Controlli e Ricerche s.r.l., Novate Milanese, Italy*

<sup>j</sup>*Now at Water and Life Lab, Entratico, Italy*

---

## Abstract

A comprehensive range of gas and particle phase pollutants were sampled at 1-hour time resolution in urban background Milan during summer 2012. Measurements include several soluble inorganic aerosols ( $\text{Cl}^-$ ,  $\text{NO}_2^-$ ,  $\text{NO}_3^-$ ,  $\text{SO}_4^{2-}$ ,  $\text{Ca}^{2+}$ ,  $\text{K}^+$ ,  $\text{Mg}^{2+}$ ,  $\text{Na}^+$ ,  $\text{NH}_4^+$ ) and gases ( $\text{HCl}$ ,  $\text{HNO}_2$ ,  $\text{HNO}_3$ ,  $\text{NH}_3$ ,  $\text{NO}$ ,  $\text{NO}_2$ ,  $\text{O}_3$ ,  $\text{SO}_2$ ), organic, elemental and black carbon and meteorological parameters. Analysis methods used include mean diurnal pattern on weekdays and Sundays, pollution roses, bivariate polar plots and statistical models using backtrajectories. Results show how nitrous acid ( $\text{HONO}$ ) was mainly formed heterogeneously at nighttime, with a dependence of its

---

Email address: pzzndr77@gmail.com (A. Piazzalunga)

formation rate on  $\text{NO}_2$  consistent with observations during the last HONO campaign in Milan in summer 1998, although since 1998 a drop in HONO levels occurred following to the decrease of its precursors. Nitrate showed two main formation mechanisms: one occurring through  $\text{N}_2\text{O}_5$  at nighttime and leading to nitrate formation onto existing particles; another occurring both daytime and nighttime following the homogeneous reaction of ammonia gas with nitric acid gas. Air masses reaching Milan influenced nitrate formation depending on their content in ammonia and the timing of arrival. Notwithstanding the low level of  $\text{SO}_2$  in Milan, its peaks were associated to point source emissions in the Po valley or shipping and power plant emissions SW of Milan, beyond the Apennines. A distinctive pattern for HCl was observed, featured by an afternoon peak and a morning minimum, and best correlated to atmospheric temperature, although it was not possible to identify any specific source. The ratio of primary-dominated organic carbon and elemental carbon on hourly  $\text{PM}_{2.5}$  resulted 1.7. Black carbon was highly correlated to elemental carbon and the average mass absorption coefficient resulted  $\text{MAC} = 13.8 \pm 0.2 \text{ m}^2 \text{ g}^{-1}$ . It is noteworthy how air quality for a large metropolitan area, in a confined valley and under enduring atmospheric stability, is nonetheless influenced by sources within and outside the valley.

*Keywords:*  $\text{PM}_{2.5}$ , hourly ionic composition, gas-phase pollutants, Po valley

---

## 1. Introduction

The interactions between gaseous and aerosol phase pollutants have long been studied due to their impact on air quality (Penkett et al., 1979; Rav-

ishankara, 1997) and on human health (World Health Organization, 2006).  
In order to investigate processes leading to atmospheric pollutants formation and ageing in densely populated areas with large emission load (i.e. hotspots), time resolved composition of both gas and particle phase atmospheric compounds are needed. Po valley (Northern Italy) is one of the most important hotspot region in Europe (Putaud et al., 2010), with Milan metropolitan area exhibiting one of the poorest air quality within the valley (Bigi and Ghermandi, 2014).

Very few 1-hour time resolution campaigns were accomplished in Milan urban area. Three noteworthy studies resulted from the Limitation of Oxidant Production/Pianura Padana Produzione di Ozono (LOOP/PIPAPPO) campaign held in May and June 1998 in Milan urban background (Neftel et al., 2002). In one of these studies Baltensperger et al. (2002) analysed data by several continuous instruments sampling aerosol physical properties (number size distribution, volatility, hygroscopicity, mass), aerosol chemical composition ( $\text{BC}_E$ , nitrate, sulphate) and two gases ( $\text{NH}_3$ ,  $\text{HNO}_3$ ). This same study showed the large contribution to airborne particles smaller than 40 nm by primary emissions rich in soot content and the increase in secondary and hygroscopic aerosol for particles larger than 50 nm. The second study within PIPAPPO, Putaud et al. (2002) collected samples of size-segregated aerosol with 4- and 7-hour time resolution and analysed them for elemental carbon (EC), organic carbon (OC), particulate organic matter (POM) and major ionic species; their results showed the large contribution ( $> 30\%$ ) to

27 PM mass by POM, by ammonium nitrate (29% of PM mass) and ammo-  
 28 nium sulphate (22% of PM mass). Putaud et al. (2002) found also a diurnal  
 29 and weekly pattern for traffic-related pollutants (e.g. EC and resuspended  
 30 mineral dust), the influence of traffic emissions on nitrate formation and of  
 31 industrial emissions on sulphate formation. In the third study of PIPAPO  
 32 Alicke et al. (2002) investigated hydroxyl radical formation by measuring  
 33 several gas phase pollutants by DOAS (Differential Optical Absorption Spec-  
 34 troscopy): HCHO, HONO, NO<sub>2</sub>, NO, O<sub>3</sub> and SO<sub>2</sub>. Their results identified  
 35 HCHO as the primary source of OH<sup>•</sup> radicals (up to 40% of total OH<sup>•</sup> on  
 36 clear days), while photolysis of nitrous acid and of ozone provides similar  
 37 contribution to atmospheric OH<sup>•</sup> (15–30% of total OH<sup>•</sup> each), with the for-  
 38 mer compound dominating during early morning and the latter during the  
 39 afternoon. In addition to the above mentioned studies, the aerosol elemental  
 40 composition and sources were investigated with hourly resolution in Milan  
 41 by D’Alessandro et al. (2003, 2004) during wintertime and summertime 2001  
 42 evidencing quasi-periodical and episodic pollution sources.

43 Several sources influence the sampling site: Bernardoni et al. (2011) used  
 44 Positive Matrix Factorization to apportion 4-hour PM<sub>10</sub> measurements and  
 45 showed the diurnal pattern in the relative contribution by resuspended dust,  
 46 construction works and industry, which altogether account for 48% to total  
 47 PM<sub>10</sub> in summer. These results were confirmed by the a detailed source ap-  
 48 portionment exercise in Milan urban background by Perrone et al. (2012),  
 49 where three years of daily PM<sub>2.5</sub> and PM<sub>10</sub> samples were analysed. This

50 latter study also showed how 60% of summer daily  $\text{PM}_{2.5}$  derives from traffic  
 51 and secondary inorganic ions (sulphate, nitrate and ammonium) and contri-  
 52 bution of resuspended dust to summer daily  $\text{PM}_{2.5}$  is only to 3.8%. Consis-  
 53 tently emission inventory for the only municipality of Milan assessed Road  
 54 Traffic (SNAP 7) to be the main source of  $\text{NO}_x$  and EC for the city of Mi-  
 55 lan, SNAP 2 (non-industrial combustion) is the main source of OC and the  
 56 second most important of  $\text{NO}_x$ , and SNAP 6 (solvent use) is the main source  
 57 of NM – VOC. Notwithstanding these studies, in Milan there is no available  
 58 analysis of simultaneous characterization of atmospheric pollutants in both  
 59 gas and particle phase sampled at a 1-hour resolution. The present article is  
 60 based on a thorough analysis of measurements of several gas phase pollutants  
 61 and main chemical composition of  $\text{PM}_{2.5}$  sampled at 1-hour time resolution.  
 62 Formation process of  $\text{PM}_{2.5}$  in Milan will be presented along with the in-  
 63 fluence of meteorological conditions and air mass trajectories. Observations  
 64 include HCl, HONO,  $\text{HNO}_3$  and  $\text{NH}_3$ , i.e. the first published measurement  
 65 of hydrochloric acid in the Po valley and the first 1-hour resolution measure-  
 66 ments of nitrous and nitric acids in the last 15 years in Milan. Details on  
 67 the instrumentation and methods used are presented in Sect. 2. Results and  
 68 conclusions are found in Sects. 3 and 4 respectively.

## 69 **2. Data and methods**

70 Milan ( $45^\circ 28' \text{N}$ ;  $9^\circ 13' \text{E}$ ) urban area counts about 1 500 000 inhabitants  
 71 and is the second largest town in Italy, after Rome, and considering the whole

72 Milan province the population rises up to about 3.1 millions inhabitants.

73 The data here presented were collected on the roof of the Department  
74 of Chemistry, University of Milan, at a  $\sim 10$  m a.g.l. within the University  
75 campus, a site representative of central urban background conditions for the  
76 city. Sampling was performed from June 5<sup>th</sup> until July 23<sup>rd</sup> 2012.

77 Hourly resolution composition of PM<sub>2.5</sub> for soluble inorganic ions compo-  
78 sition and for gases was determined using a commercially available Ambient  
79 Ion Monitor (AIM) URG-9000D (URG Corp, USA). In particle phase five  
80 anions ( $\text{Cl}^-$ ,  $\text{F}^-$ ,  $\text{NO}_2^-$ ,  $\text{NO}_3^-$ ,  $\text{SO}_4^{2-}$ ) and five cations ( $\text{Ca}^{2+}$ ,  $\text{K}^+$ ,  $\text{Mg}^{2+}$ ,  $\text{Na}^+$ ,  
81  $\text{NH}_4^+$ ) were determined.  $\text{F}^-$ ,  $\text{Ca}^{2+}$ ,  $\text{K}^+$ ,  $\text{Mg}^{2+}$  and  $\text{Na}^+$  were often below the  
82 detection limit and therefore not analysed in details. The gases determined  
83 include hydrochloric acid (HCl), nitrous acid (HONO), nitric acid ( $\text{HNO}_3$ ),  
84 ammonia ( $\text{NH}_3$ ) and sulphur dioxide ( $\text{SO}_2$ ). The AIM consists of a sampling  
85 system for both gas and particles, coupled with two ion chromatographies for  
86 the analytical determination. Gases are collected by a liquid diffusion denun-  
87 der with  $\text{H}_2\text{O}_2$  5 mM running continuously at  $10 \text{ mL h}^{-1}$  flow rate. Particles  
88 are collected in a chamber supersaturated with ultrapure water vapour: wa-  
89 ter soluble particles are allowed to grow and then inertially separated and  
90 injected into the ion chromatographies. Further instrumental details and  
91 the calibration procedure used in this study can be found in Markovic et al.  
92 (2012). AIM data were compared to off-line daily data from PM<sub>2.5</sub> samples  
93 collected during 22 days throughout the campaign by denuded filter-pack  
94 setup (Vecchi et al., 2009): the system consisted in two dry annular denud-

95 ers removing both acidic and basic gases, followed by a filter pack made of a  
 96 quartz fibre front filter and a nylon fibre backup filter. Once the campaign  
 97 ended, AIM blank values for particle-phase aerosol were estimated by insert-  
 98 ing a quartz fibre filter between the denuder and the filter pack over 5 full  
 99 days.

100 Comparison of AIM and denuded filter pack showed statistically significant  
 101 (by ANOVA test) and large coefficients of determination for linear regression  
 102 models between off- and on-line data for all species (Figure S1), supporting  
 103 the reliability of the patterns observed by AIM. Regression coefficients were  
 104 close to unity for  $\text{HNO}_2 + \text{HNO}_3$  and  $\text{NH}_3$ , while some difference occurred be-  
 105 tween particle-phases compounds, with lower  $\text{NO}_2^- + \text{NO}_3^-$  levels observed by  
 106 AIM and lower values for  $\text{SO}_4^{2-}$  and  $\text{NH}_4^+$  observed by denuded filter-pack.  
 107 Assuming that the denuded filter pack reported in Vecchi et al. (2009) is  
 108 artefact-free for nitrogen compounds, some bias likely affects ammonium in  
 109 AIM measurements, preventing a fully-correct estimate of ion balance for  
 110 the experimental dataset. Part of the offset between the two measurement  
 111 sets might also be due to the possibly different transmission efficiency curve  
 112 between respective size-selective inlets: AIM uses a custom  $\text{PM}_{2.5}$  cyclone,  
 113 while denuded filter pack used a US-EPA equivalent  $\text{PM}_{2.5}$  inlet equipped  
 114 with a  $\text{PM}_{10}$  sampling head and a WINS  $\text{PM}_{2.5}$  impactor downstream.

115 Gaseous precursors levels during AIM blank test resulted similar to their re-  
 116 spective mean observed during the campaign, indicating an efficient collection  
 117 of gas and a complete transmission of particles by the denuders. Significant



118 particulate sodium was observed during blanks and ascribed to contamina-  
119 tion in the ultrapure water used in the supersaturated chamber during the  
120 blank test. The low particulate nitrite, nitrate and ammonium observed  
121 during blank testing (i.e.  $< 1 \mu\text{g m}^{-3}$ ) can be considered negligible. Slightly  
122 larger blank for particulate sulphate was observed ( $\sim 1.5 \mu\text{g m}^{-3}$ ), but con-  
123 sidered sufficiently low to support the reliability of the AIM measurements  
124 for this compound.

125 Elemental carbon (EC) and organic carbon (OC) measurements were col-  
126 lected by a Model-4 Semi-Continuous ECO-C Field Analyser by Sunset Lab-  
127 oratory, USA (Bae et al., 2004). The carbon analyser was provided with  
128 a  $\text{PM}_{2.5}$  cyclone and operated at a  $24 \text{ L min}^{-1}$  flowrate. Measurement had  
129 1-hour time resolution, comprising 45 minutes for sampling and 15 minutes  
130 for thermal-optical analysis. The analysis followed a high temperature ana-  
131 lytical protocol featured by 2 steps in inert atmosphere ( $625^\circ\text{C}$ ,  $870^\circ\text{C}$ ) and  
132 3 steps in oxidizing atmosphere ( $650^\circ\text{C}$ ,  $675^\circ\text{C}$ ,  $870^\circ\text{C}$ ). During most of the  
133 campaign the split point (i.e. the separation between OC and EC) occurred  
134 in inert atmosphere: the pre-combustion of EC was attributed to the low  
135 carbon amount and to the presence of undesired oxygen or of metal oxides  
136 accumulated on the filter. The data analysis included only EC-OC measure-  
137 ment having a split point above  $650^\circ\text{C}$  (Jung et al., 2011), in accordance  
138 with EUSAAR2 protocol for off-line laboratory measurements (Cavalli et al.,  
139 2010). Both calibration and filter replacement were performed on a weekly  
140 basis; no EC-OC data are available on Sundays.

141 Aerosol light absorption coefficient ( $\sigma_{\text{ap}}$ ) was measured by a Multi-Angle  
142 Absorption Photometer (MAAP, model 5012, Thermo Scientific Corp., USA)  
143 equipped with a  $\text{PM}_{2.5}$  inlet. Atmospheric equivalent black carbon concen-  
144 tration ( $\text{BC}_{\text{E}}$ ) is estimated by the instrument using a MAC (mass specific  
145 absorption cross section) of  $6.6 \text{ m}^2 \text{ g}^{-1}$  (Petzold et al., 2002).  $\text{BC}_{\text{E}}$  measure-  
146 ments had a 5-min resolution and the data were then averaged to 1 hour. To  
147 evaluate atmospheric dispersion conditions,  $^{222}\text{Rn}$  short-lived decay products  
148 measurements were performed using the experimental methodology reported  
149 in Marcazzan et al. (2003). Hourly measurements of meteorological param-  
150 eters (wind speed and direction, temperature, relative humidity, pressure,  
151 global solar radiation and precipitation) were sampled on the roof of the De-  
152 partment of Physics, University of Milan, at  $\sim 10 \text{ m a.g.l.}$ , within the grounds  
153 of the University campus. Concentration of  $\text{NO}$ ,  $\text{NO}_2$  and  $\text{O}_3$  were provided  
154 by an urban background station sited 400 m NE of the campus and within  
155 the air quality monitoring network of the Regional Environmental Protection  
156 Agency of Lombardy (ARPA).

157

158 A tentative localization and identification of the pollution sources was  
159 performed by four techniques: analysis of conditional bivariate probability  
160 function (CBPF), bivariate polar plots, air mass origin by simulated back-  
161 trajectory and backtrajectory statistical models (BSMs). The former two  
162 techniques are headed to identify local sources, while backtrajectories were  
163 used to potentially track pollution events due to distant sources. CBPF

164 technique estimates the probability that a specific concentration range is  
 165 observed within a given wind sector, depending upon wind speed (more de-  
 166 tails in Uria-Tellaetxe and Carslaw, 2014). Bivariate polar plots (Carslaw  
 167 and Ropkins, 2012) are a level plot in polar coordinates where colour scale  
 168 represents pollutant concentration and polar coordinates are a smoothed in-  
 169 terpolation of wind speed and wind direction by Generalised Additive Model  
 170 (Wood, 2006). Origin of air masses arriving in Milan at 100 m a.g.l. was esti-  
 171 mated with 36-hours long backtrajectories simulated by HYSPLIT (Draxler  
 172 and Rolph, 2013) using 0.5° GDAS meteorological data. 24 trajectories per  
 173 day were computed, i.e. one per hour. The statistical models applied to back-  
 174 trajectories include Concentration Field (CF), Potential Source Contribution  
 175 Function (PSCF) and Gridded Difference (GD) using respective functions in  
 176 Carslaw and Ropkins (2012). All of the three attempt to combine trajectory  
 177 path to concentration at the receptor; further details about BSMs can be  
 178 found in Carslaw and Ropkins (2012) and Fleming et al. (2012). Scheifinger  
 179 and Kaiser (2007) proved BSMs to provide useful information on potential  
 180 source areas only for distances within the mean residence time of the inves-  
 181 tigated compound; for trajectories longer than this period the effect of tur-  
 182 bulent dispersion and removal processes, neglected by the statistical models  
 183 and the backtrajectories, may lead to unreliable results (Han et al., 2005). In  
 184 the present study trajectory statistical models were tested for several species,  
 185 although significant results occurred only for SO<sub>2</sub>, SO<sub>4</sub><sup>2-</sup> and NH<sub>3</sub>. For sul-  
 186 phur dioxide Scheifinger and Kaiser (2007) suggest to limit backtrajectories

187 within 60 hours: in this study a length of 36 hours (i.e. largely within 60  
188 hours) was used for all pollutants.

189

190 Few different emission inventories were used to review BSM outputs and  
191 to identify realistic potential sources: a plot pairing inventory database and  
192 corresponding area is presented in Figure S2. Emission inventories for Lom-  
193 bardy, Piedmont and Veneto were consistently compiled (INEMAR, 2015),  
194 resulting in a bottom-up inventory with a spatial resolution at the municipal-  
195 ity district level. These inventories are compliant to the EMEP-CORINAIR  
196 guidebook, the IPCC guidelines and the Good Practice Guidance, they are  
197 classified accordingly to SNAP (Selected Nomenclature for Air Pollution)  
198 and the emission data used in this study refers to 2010 for Lombardy and  
199 2008 for Piedmont and Veneto. Emissions for Aosta Valley, Liguria, Rhône  
200 Alpes and Provence-Alpes-Côte d’Azur refers to 2008, have a spatial res-  
201 olution at the municipality district level and include point sources for the  
202 three former regions. Data were provided by the project AERA (Air Envi-  
203 ronnement Regions ALCOTRA) through a Web Map Service (AERA, 2015).  
204 Finally, emissions for all other regions involved in this study were provided  
205 by the UNECE/EMEP emission inventory for 2012. Accuracy and uncer-  
206 tainty of these inventories are different, as well as the procedure to build  
207 them, their spatial resolution and their reference year. In this study inven-  
208 tories were used to identify areas with significant SO<sub>2</sub> emissions (e.g. large  
209 industrial plants) and to approximately compare potential sources, therefore

210 the discrepancies between these databases were considered negligible for the  
211 purpose of this analysis. Nonetheless the closer the investigated area is to  
212 Milan, the more detailed is the inventory used, allowing a reliable analysis  
213 of nearby and directly impacting sources.

214 All statistical data analyses were performed within the software environ-  
215 ment R 3.0.2 (R Core Team, 2013). All data are reported in local time, i.e.  
216 Central European Summer Time (CEST).

### 217 **3. Results and discussion**

218 In the following the data will be presented and discussed in specific sub-  
219 sections for each common species, including their pattern, formation and  
220 removal processes (if known) and their potential source. The analysis inves-  
221 tigate the average concentration pattern over the whole sampling period,  
222 and the variability of a subset of pollutants under different atmospheric dis-  
223 persion conditions.

#### 224 *3.1. Meteorological setting*

225 June and July 2012 were featured by high pressure fields originated by the  
226 Azores high and occasionally by subtropical anticyclones (Figure S3). Large  
227 values of mean geopotential height at 500 hPa occurred during the sampling  
228 campaign, when June was characterized by anticyclonic curvature and mod-  
229 erately positive anomaly and July by a slightly cyclonic curvature. This  
230 meteorological context determined recurrent atmospheric stability, clear-sky

231 and high temperatures, enhancing photochemical activity and formation of  
 232 tropospheric ozone. Hot weather conditions occurred between the end of  
 233 June and the beginning of July and, after a short instability period, since  
 234 July 8<sup>th</sup>. Main meteorological events reducing atmospheric pollutants levels  
 235 occurred at the beginning of June prompted by moderately perturbed fluxes  
 236 and Atlantic cold fronts, on the 14<sup>th</sup> and 15<sup>th</sup> of July due to ventilation orig-  
 237 inated by a temporary positioning in the North of Alps of the maximum of  
 238 the Azores high, and on July 21<sup>st</sup> when a cold front led to intense rainstorms  
 239 in Milan and surroundings. A mountain-valley breeze regime was present  
 240 during large part of the campaign, with low N winds at night ( $< 2 \text{ m s}^{-1}$ ),  
 241 increasing and rotating at daytime until a SW flow is established in the af-  
 242 ternoon with speeds up to  $4 \text{ m s}^{-1}$ . These meteorological conditions were  
 243 typical of summers in Northern Italy, therefore notwithstanding measure-  
 244 ments did not cover the whole summer, they are well representative of the  
 245 entire season. A summary of statistical values for the measured parameters  
 246 is presented in table B.1. In Figure B.1 the diurnal pattern during weekdays  
 247 and Sundays are presented for several observed pollutants, along with tem-  
 248 perature (T), Radon concentration (Rn), global radiation (GR) and relative  
 249 humidity (RH).

### 250 3.2. Nitrogen oxides and ozone

251 Nitric oxide shows sharp peaks at mornings only on weekdays, indicating  
 252 a source from rush hour traffic, along with relatively low atmospheric mixing;

253 NO rapidly declines due to vertical mixing and its oxidation to  $\text{NO}_2$  by  $\text{O}_3$   
254 and by the available radical groups.

255 Nitrogen dioxide peaks at morning rush hours. The afternoon decrease  
256 in  $\text{NO}_2$  is driven by 3 processes: dilution due to the rise in mixing layer  
257 height, photolysis to NO under intense solar radiation and reaction with  $\text{OH}\cdot$   
258 to nitric acid. The difference between weekdays and Sundays is noteworthy  
259 for both NO and  $\text{NO}_2$ , strongly indicating an anthropogenic source, most  
260 likely traffic, of these compounds.

261 Ozone shows an afternoon peak generated by the large availability of  
262  $\text{OH}\cdot$  radicals and possibly by the re-entrainment of  $\text{O}_3$  within the residual  
263 layer (Zhang and Trivikrama Rao, 1999). Indeed the sum of  $\text{NO}_2$  and  $\text{O}_3$   
264 shows a slightly higher peak on weekdays indicating the small contribution  
265 by fresh emissions to oxidant species. Ozone exhibits a very mild weekend  
266 effect (Cleveland et al., 1974; Jiménez et al., 2005; Tonse et al., 2008; Pollack  
267 et al., 2012; Wang et al., 2014), e.g. higher mixing ratios on Sundays due  
268 to lower  $\text{NO}_x$  emissions over the weekend and therefore reduced titration  
269 of  $\text{O}_3$ , as shown for Milan by Vecchi and Valli (1999). Since 1700 CEST  
270 mixing decreases leading to an increase in  $\text{NO}_x$  and a drop in ozone. Diurnal  
271 pattern for  $\text{NO}_x$  and  $\text{O}_3$  are highly similar to mean diurnal pattern for long  
272 term measurements in Modena, 160 km SE of Milan, Po valley (Bigi et al.,  
273 2012), where ozone exhibits also similar levels to those observed in Milan,  
274 consistently with the atmospheric homogeneity across the valley.

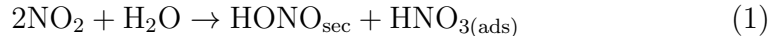
### 275 3.3. Nitrous acid and nitrites

276 Gas-phase nitrous acid (HONO) shows a pattern similar to past obser-  
 277 vations in Milan by Stutz et al. (2002) and Febo et al. (1996), featured by  
 278 lower mixing ratios at daytime, due to photolysis, and peak at nighttime,  
 279 most likely by heterogeneous formation. Particle-phase nitrites ( $\text{NO}_2^-$ ) ex-  
 280 hibit a diurnal pattern highly similar to HONO, as observed in Marseille  
 281 (Acker et al., 2005), suggesting that part of atmospheric HONO is formed  
 282 heterogeneously onto particle surfaces under high RH conditions. Traffic  
 283 emissions are another possible source of HONO: Kurtenbach et al. (2001)  
 284 found large variability in the ratio  $\text{HONO}/\text{NO}_x$  from road tunnel measure-  
 285 ments depending on fuel, emission control systems and motor load. A ratio  
 286 for  $\text{HONO}/\text{NO}_x$  of 1 % was used in this study, similarly to the ratio used  
 287 by Michoud et al. (2014) for Paris and higher than 0.65 % as used by Stutz  
 288 et al. (2002) for Milan. In order to remove HONO direct emissions from total  
 289 HONO, secondary HONO was estimated as  $\text{HONO}_{\text{sec}} = \text{HONO} - 0.01 \cdot \text{NO}_x$ ,  
 290 resulting in a  $\sim 80$  % of total HONO from secondary origin.

291 Main formation mechanism of  $\text{HONO}_{\text{sec}}$  in urban atmosphere is expected  
 292 to proceed heterogeneously onto surfaces, following reactions 1 and 2, with  
 293 1 being the most likely process (Kleffmann, 2007). It is still unclear whether  
 294 the contribution of heterogeneous formation of  $\text{HONO}_{\text{sec}}$  onto soot particles  
 295 (Kalberer et al., 1999) is a significant source to atmospheric concentrations  
 296 (Kleffmann, 2007; Ziemba et al., 2010) or not (Finlayson-Pitts and Pitts,



297 2000).



298



299 Latest published measurements of nitrous acid in Milan urban background  
 300 were collected in May and June 1998 by Alicke et al. (2002) and Stutz et al.  
 301 (2002). The latter investigated HONO formation by DOAS-resolved vertical  
 302 profiles and found that  $\text{HONO}_{\text{sec}}$  was formed at ground. Stutz et al. (2002)  
 303 estimated that 1 molecule of  $\text{HONO}_{\text{sec}}$  was released each 25–40 molecules of  
 304  $\text{NO}_2$  and assessed the  $\text{NO}_2$  conversion efficiency to be an order of magnitude  
 305 lower than expected according to reaction 1.

306 In Alicke et al. (2002) HONO mixing ratios by DOAS exhibited a night-  
 307 time and daytime mean of 0.92 ppb and 0.14 ppb respectively. In summer  
 308 2012 the mean mixing ratios observed were of 0.6 ppb at nighttime and  
 309 0.5 ppb at daytime, with the latter being largely higher than in 1998 and  
 310 potentially biased by artefacts. Maximum nitrous acid levels were similar in  
 311 both studies: 4.4 ppb and 4.2 ppb in 1998 and 2012 respectively.

312 In order to assess whether a long term trend in HONO is present and  
 313 2012 daytime data are artefact-freefall, an analysis of  $\text{NO}_2$  levels from 1998  
 314 through 2012 was performed. Mean daytime  $\text{NO}_2$  concentration during the  
 315 two sampling campaigns were 18.3 ppb and 4.9 ppb in 1998 and 2012 re-  
 316 spectively, while mean nighttime  $\text{NO}_2$  concentration was 33.2 ppb in 1998  
 317 and 8.8 ppb in 2012. These observations are consistent with an estimated

318 long term trends for deseasonalized monthly mean concentration of  $\text{NO}_2$  of  
 319  $-1.47 \pm 0.17 \text{ ppb yr}^{-1}$  (trends are estimated by Generalised Least Squares  
 320 method as in Bigi and Ghermandi (2014)). Given the large  $\text{NO}_2$  concentra-  
 321 tions in 1998, Stutz et al. (2002) found a large contribution of direct emissions  
 322 to atmospheric HONO, notwithstanding they made use of a low  $\text{HONO}/\text{NO}_x$   
 323 ratio, i.e. 0.65%. The large decrease in  $\text{NO}_2$  from 1998 to 2012 should cause  
 324 a significant decrease in HONO over the same period, although, according to  
 325 2012 HONO data, a decrease occurred only at nighttime. Several intercom-  
 326 parison studies of HONO measurements by DOAS and chemical instruments  
 327 (e.g. wet denuder and LOPAP) showed how results from different techniques  
 328 agreed well at nighttime, while HONO by standard wet denuders might suf-  
 329 fer from positive artefacts at daytime (Kleffmann et al., 2006): these might  
 330 occur by reaction on denuder surface either of semivolatile diesel exhausts  
 331 with  $\text{NO}_2$  (Gutzwiller et al., 2002), either of pure  $\text{NO}_2$  (Kleffmann et al.,  
 332 2006), either of  $\text{NO}_2$  and  $\text{S(IV)}$  (Spindler et al., 2003). The high HONO and  
 333  $\text{HONO}_{\text{sec}}/\text{NO}_2$  ratio in 2012 at daytime suggest that 2012 daytime HONO  
 334 mixing ratios might be biased by a chemical interference in the denuder, since  
 335 are not consistent with the observed decrease in  $\text{NO}_2$  from 1998 to 2012 and  
 336 the corresponding decrease in nighttime HONO over the same period.

337 Assuming that during nighttime most of nitrous acid is formed through  
 338 reaction 1, which is first order in  $\text{NO}_2$ , formation rate between two generic

instants  $t_1$  and  $t_2$  was computed according to equation 3.

$$\overline{F_{HONO_{sec}}} = \frac{[HONO_{sec}](t_2) - [HONO_{sec}](t_1)}{(t_2 - t_1)[NO_2]_{night}} \quad (3)$$

Formation rate is best estimated for nights when NO and NO<sub>2</sub> levels are low, in order to consider negligible both direct HONO emissions by traffic and positive artefacts, and when HONO formation is steady and lasts throughout the night, in order to average over several hours. These conditions are met between June 18<sup>th</sup>–19<sup>th</sup>, since NO and NO<sub>2</sub> concentration were steadily below 5 ppb and 15 ppb (Figure B.2), and lead to a formation rate of 0.009 ppb HONO<sub>sec</sub>/ (h (ppb NO<sub>2</sub>)), consistently with the rate of (0.012±0.005) found by Alicke et al. (2002) in Milan by DOAS.

#### 3.4. Nitric acid, nitrates and ammonia

Nitric acid is formed by reaction of OH· with NO<sub>2</sub> leading to HNO<sub>3</sub> characteristic pattern featured by a single afternoon peak, when hydroxyl radicals are abundant. Nitric acid formation is expected to be controlled by the availability of OH· rather than by NO<sub>2</sub>, since HNO<sub>3</sub> diurnal pattern exhibits no difference between weekdays and Sundays, contrarily to NO<sub>2</sub>, whose peak is above 12 ppb on weekdays and ~5 ppb on Sundays.

Atmospheric particle nitrate is expected to be formed by two main pathways, either through reaction of HNO<sub>3</sub> with NH<sub>3</sub> or through absorption of N<sub>2</sub>O<sub>5(g)</sub> (Lammel and Cape, 1996; Finlayson-Pitts and Pitts, 2000): the former reaction is homogeneous, the latter is heterogeneous and occurring only

359 at slow rates and at nighttime, since  $\text{N}_2\text{O}_5$  and  $\text{NO}_3$  photolyse very rapidly  
360 (see Appendix A). The heterogeneous pathway is expected to form signifi-  
361 cant amount of aerosol nitrate: Alexander et al. (2009) estimated a similar  
362 contribution by the two pathways on an annual basis in Italy, while Michalski  
363 et al. (2003) estimated the heterogeneous pathway to contribute up to 50%  
364 to total summer nitrate in La Jolla (Southern California).

365 Diurnal pattern of nitrate shows an increase since 0200 to 1000 CEST dur-  
366 ing weekdays, whereas on Sundays exhibits steady concentration at mornings  
367 and an increase since 0900 to 1400 CEST. Afternoon patterns do not differ  
368 both in shape and levels between weekdays and Sundays. Two methods were  
369 used to investigate partitioning of ammonium nitrate with its precursors  
370 at thermodynamic equilibrium: ISORROPIA 2.1 (Fountoukis and Nenes,  
371 2007) simulation model (forward mode and thermodynamically stable state  
372 conditions) and dissociation constants for reaction A.2 of ammonium nitrate  
373 aerosol assuming a single-component aerosol (see Appendix B for details and  
374 calculations). Both methods show how patterns of atmospheric nitrate and  
375 theoretical partitioning do not fully match (Figure S4), differently to other  
376 continental climate sites in summer (e.g. Melpitz, Germany (Poulain et al.,  
377 2011)), suggesting that condensation/evaporation processes do not exclu-  
378 sively control aerosol nitrate.

379 At nighttime  $\text{N}_2\text{O}_5$  is expected to be partly responsible of the nitrate  
380 increase, also suggested by the slower formation rate compared to the one  
381 required by the thermodynamic equilibrium of the homogeneous reaction ac-

382 cording to ISORROPIA (not shown). The nitrate increase after sunrise is  
 383 possibly kept up by homogeneous reaction A.2, triggered by the rapid forma-  
 384 tion of nitric acid from  $\text{NO}_2$  rush hour emissions: since there is no evidence of  
 385 nitric acid rise until 0900–1000, possibly this early morning  $\text{HNO}_3$  is rapidly  
 386 converted to nitrate. On Sundays nitrate increases from 0900–1000, i.e. most  
 387 likely through the diurnal homogeneous reaction: the lower  $\text{NO}_2$  levels over  
 388 the weekend (Saturday and Sunday) lead to a smaller production of early  
 389 morning  $\text{HNO}_3$  and nighttime  $\text{N}_2\text{O}_5$ . Nitrate decreases during afternoons  
 390 due to temperature increase and the shift of ammonium nitrate equilibrium  
 391 to the gas-phase. Occasional morning increase in nitrate might be due also  
 392 to re-entrainment of nitrate within the residual layer, which has been shown  
 393 to provide a significant contribution to ground level concentration in Milan  
 394 in summer (Curci et al., 2015).

395 Diurnal pattern for ammonia shows a steady profile. This is due to sev-  
 396 eral reasons: total  $\text{NH}_3 + \text{NH}_4^+$  is mainly in gasphase ammonia, therefore the  
 397 particulate phase is not significantly affecting  $\text{NH}_3$  concentration. Variability  
 398 in aerosol nitrate diurnal pattern is almost negligible compared to ammonia  
 399 levels, therefore no significant amount of ammonia is expected to be released  
 400 in the afternoon when ammonium nitrate equilibrium moves towards gas-  
 401 phase. Besides, in the afternoon  $\text{HNO}_3$  increases, leading to ammonium ni-  
 402 trate formation partly compensating the dissociation of ammonium nitrate.  
 403 Sulphate shows quite constant concentration and no significant change in  
 404  $\text{NH}_3$  is expected from ammonium sulphate. Finally  $\text{NH}_3$  emissions might

405 be slightly larger during daytime, but compensated by dilution from the  
406 enhanced boundary layer.

407       CBPF for nitrate shows how peak concentration of this compound is as-  
408 sociated to very low wind speeds, i.e. is formed locally and concentrations  
409 increase due to the low dispersion conditions. On the contrary, median to  
410 moderate nitrate concentrations are associated to S or SSE winds, i.e. winds  
411 associated to moderate-large ammonia content. CBPF for ammonia indi-  
412 cates that larger observed levels are associated to distant sources at S, SSE,  
413 E and W of Milan, most likely emissions from agricultural activities in the  
414 Po valley surrounding the city. The existence of farther sources of ammo-  
415 nia were investigated also by BSMs (see Figure S5), which confirm emissions  
416 within the Po valley as main responsible for ammonia levels in Milan. This is  
417 consistent with 2010 emission inventories, ascribing 97% of all ammonia emis-  
418 sions to agricultural activities, and the remainder to traffic and wastewater  
419 treatment (Bigi and Ghermandi, under review).

420       During the campaign, significant pollution episodes occurred, both for  
421 particulate nitrate (June 8<sup>th</sup>–9<sup>th</sup>) and ammonia (June 27<sup>th</sup>–28<sup>th</sup>). The former  
422 occurred during a 48-hours period of relatively low temperature featured by a  
423 blocked atmosphere and an elevated inversion (Figure S6), the latter occurred  
424 during a rapid transport of ammonia originated in the Po valley (Figure S7).

### 425 3.5. *Hydrochloric acid*

426 Known anthropogenic sources of HCl are coal combustion (Lightowlers  
427 and Cape, 1988), biomass burning and waste incineration (Kaneyasu et al.,  
428 1999), whereas main natural source of HCl is sea-salt (Eldering et al., 1991).  
429 Few measurements of atmospheric HCl mixing ratios are reported in the  
430 literature and the data here presented are the first published measurements in  
431 Milan, to authors knowledge. Mean HCl level during the campaign resulted in  
432 0.19 ppb. In summer 1999 Bari et al. (2003) observed 0.32 ppb and 0.28 ppb of  
433 HCl in two areas within New York City and attributed it to sea-salt. Eldering  
434 et al. (1991) observed HCl mixing ratios up to 3 ppb in Southern California in  
435 summer 1986 and demonstrated its formation by sea-salt chloride depletion  
436 by attack of  $\text{HNO}_3$ . Kaneyasu et al. (1999) showed the contribution of waste  
437 incineration to both atmospheric HCl and aerosol chloride during winter  
438 1991 in the Japanese Kanto Plain, where chloride ranged between  $10 \mu\text{g m}^{-3}$   
439 and over  $70 \mu\text{g m}^{-3}$ . The study by Kaneyasu et al. (1999) showed how HCl  
440 emissions combined with  $\text{NH}_3$  to  $\text{NH}_4\text{Cl}_{(\text{p})}$ , which finally dissociate to gaseous  
441 HCl and  $\text{NH}_3$  at daytime with warmer atmospheric temperatures.

442 Observed HCl in Milan exhibits no weekly pattern, but a clear diurnal  
443 pattern identically repeated throughout the week and best correlated to at-  
444 mospheric temperature (see Figure B.1). This outcome was confirmed by  
445 a bivariate polar plot analysis conditioning concentration on atmospheric  
446 temperature instead of wind speed, indicating that higher HCl values are  
447 associated to higher temperature and do not depend on wind direction (Fig-

ure B.3). Atmospheric temperature is higher in the afternoons, when a SW breeze is established, explaining why in Figure B.3 larger HCl is associated to SW winds. The presence of a significant distant source (e.g. sea) for HCl was checked by BSMs, which pointed to a near source, excluding long range transport (see Figure S8). Similarly, the analysis of sodium chloride balance, considering both aerosol and gas phase, resulted in a large excess in Chlorine. These outcomes suggest that HCl is originated by a chlorinated compound free to evaporate in the atmosphere from a non-point source, and sufficiently abundant to generate significant atmospheric HCl levels. Unfortunately available data are not sufficient to explain this excess in Chloride and further samplings are needed to unveil the origin of HCl.

### 3.6. Sulphur dioxide and sulphates

SO<sub>2</sub> concentration in Milan are similar to other European cities (see Henschel et al., 2013, for an European overview) and its diurnal pattern, along with that of sulphate, shows no distinctive features, besides slightly lower concentrations on Sundays. Few stationary sources of SO<sub>2</sub> have significant emissions and are sufficiently near Milan to directly impact the city: the largest is an industrial area including a refinery and a carbon black manufacture sited 40 km West of the sampling site and emitting altogether  $\sim 6\,900\text{ Mg yr}^{-1}$  of SO<sub>2</sub> (E1 in Figure B.4). Other significant SO<sub>2</sub> sources are: a refinery sited 50 km South-West of the sampling site, with an estimated SO<sub>2</sub> emission of  $4\,500\text{ Mg yr}^{-1}$  (E2 in Figure B.4) and a refinery sited



130 km ESE (annual SO<sub>2</sub> emission of 1 600 Mg) (E3 in Figure B.4).  
 CBPF, bivariate polar plots and trajectory statistical models were used to  
 identify whether any of the above potential source is impacting the sampling  
 site. CBPF analysis associates low SO<sub>2</sub> levels (0.0–0.5 ppb, i.e. below the  
 20th quantile) to Northerly winds (CBPF plots for SO<sub>2</sub> are in Figure S9).  
 Moderate SO<sub>2</sub> concentrations (20th–70th quantile) are associated to a South-  
 ern source (possibly E1 and/or Genoa) and a Western source (possibly E2).  
 Highest concentrations are associated to a source SW of the site, most likely  
 E1. Consistently bivariate polar plot for SO<sub>2</sub> associates mean levels to W  
 and SW winds (Figure B.5e).

Potential sources of long-range transported SO<sub>2</sub> identified by BSMs were  
 nearby Venice (250 km E of Milan) and in the Ligurian Sea/Ligurian shore  
 (Figure S10). At the former a large refinery and a power plant are present;  
 at the latter SO<sub>2</sub> emissions are expected by ship traffic and by a power plant  
 (E4 in Figure B.4) which is partly coal fired. Finally some contribution could  
 occur by sources nearby Marseille (E5 in Figure B.4), where an overall SO<sub>2</sub>  
 emissions in the order of 50 000 Mg yr<sup>-1</sup> is expected.

Regarding sulphate, CBPF associates its lowest concentration to Northerly  
 winds (see Figure S11), similarly to SO<sub>2</sub>. Low sulphate concentration is as-  
 sociated to low Eastern winds, possibly aged emissions from Venice or E3.  
 Median sulphate levels (SO<sub>4</sub><sup>2-</sup> ranging between 4.1–5.4 µg m<sup>-3</sup>, i.e. between  
 40th–60th quantile) are associated to moderate SW winds, suggesting a dis-  
 tant origin, eventually E4. Peaks in sulphate are associated to low SW winds

493 and possibly originate from E1 emissions. Backtrajectories models for sul-  
 494 phate suggest possible sources similar to SO<sub>2</sub> (Figure S12): all three statisti-  
 495 cal models indicate a source in the Ligurian sea, most likely maritime traffic  
 496 and E4, a source nearby Venice and possibly some contribution from the area  
 497 of Marseille. BSMs results consider transport from closer sources, within 36  
 498 hours travel distance: SO<sub>2</sub> oxidation rate for coal-fired power plant plume in  
 499 summer was estimated as  $\sim 1\% \text{ h}^{-1}$  (Richards et al., 1981). Therefore the  
 500 presence of other (e.g. more distant) sources of sulphate impacting Milan is  
 501 possible, although their identification would require backtrajectories longer  
 502 than 36 hours, better if associated to a particle dispersion model in order to  
 503 provide reliable results for a BSMs (Han et al., 2005, e.g.) and beyond the  
 504 aims of this study.

### 505 *3.7. Elemental, organic and black carbon*

506 EC exhibits a typical diurnal pattern of primary pollutants on weekdays,  
 507 with a peak at 0800 CEST and a minimum when atmospheric mixing is high-  
 508 est. OC diurnal pattern on weekdays is featured by a slight afternoon increase  
 509 due to secondary aerosol formation. The diurnal pattern for OC/EC ratio  
 510 during weekdays, an index of secondary organic carbon formation, shows a  
 511 minimum during primary emissions and a maximum during intense photo-  
 512 chemical activity. No EC and OC data are available for Sundays. Following  
 513 the rationale of Cabada et al. (2004), the EC tracer method was used to  
 514 estimate secondary-influenced and primary-dominated OC, OC<sub>s</sub> and OC<sub>p</sub>

515 respectively. Hours with lower photochemical activity were selected upon  
 516 ozone levels: for each day the 25th quantile of Ozone was computed and  
 517 only OC EC data during hours with Ozone below this threshold have been  
 518 used to estimate the  $OC_p$  to EC regression. Some limitations apply to this  
 519 simplistic rationale for the Po valley, where large levels of SOA are expected  
 520 even at low ozone concentration. The primary-dominated OC to EC linear  
 521 fit resulted in a slope of 1.7 and an intercept of  $2.9 \mu\text{g m}^{-3}$  (Figure B.6),  
 522 similarly to the ratio of 1.7 found by Lonati et al. (2007) for summer 2002  
 523 and 2003 on daily  $PM_{2.5}$  samples in Milan. The intercept most likely includes  
 524 sampling artefacts, non-combustion OC emissions (e.g. biogenic), meatcook-  
 525 ing operations and background OC. These coefficients were used to estimate  
 526 secondary organic aerosol (SOA) concentration and finally CBPF was used  
 527 to estimate potential transport. Results show how peak SOA values are asso-  
 528 ciated to winds from the SW sector, i.e. to afternoon winds with maximum  
 529 solar radiation and photochemical activity. Median concentration of SOA  
 530 are associated to Easterly winds, most likely transported from OC emissions  
 531 within the Po valley.

532 Absorption coefficient by MAAP is well correlated to EC, leading to an  
 533 average mass absorption coefficient  $MAC = 13.8 \pm 0.2 \text{ m}^2\text{g}^{-1}$ , in fair agree-  
 534 ment to previous studies on off-line quartz fibre filters sampled in Milan  
 535 (Vecchi et al., 2012). MAC is fairly constant throughout the day, with a day-  
 536 time  $MAC_{\text{day}} = 13.5 \pm 0.3 \text{ m}^2\text{g}^{-1}$  and night-time  $MAC_{\text{night}} = 13.9 \pm 0.3 \text{ m}^2\text{g}^{-1}$   
 537 (Figure S13), indicating the same EC source, most likely traffic.

538  $\text{BC}_\text{E}$  and EC, along with nitric oxide, show similar bivariate polar plots  
539 indicating a nearby main source sited SSE, along the direction of the nearest  
540 major road (see Figure B.5b for  $\text{BC}_\text{E}$ ). CBPF associates lower concentration  
541 in  $\text{BC}_\text{E}$  and EC to SW winds, because of the dispersion induced by the stronger  
542 SW afternoon winds.

#### 543 4. Conclusions

544 The article presented the most recent and complete analysis of 1-hour  
545 resolution observations of gaseous pollutants and main chemical composition  
546 of  $\text{PM}_{2.5}$  in Milan. Ozone and nitrogen oxides pattern are consistent with  
547 intense photochemical activity under strong solar radiation, heavy emission  
548 sources and recirculation of pollutants, along with re-entrainment from the  
549 residual layer. HONO mixing ratios, compared to 1998, exhibited a de-  
550 crease, consistently with the reduction in  $\text{NO}_2$  atmospheric concentration,  
551 although with a similar formation rate. Particulate nitrate formed through  
552 two pathways, depending upon the meteorological conditions and air mass  
553 origin. Backtrajectories and pollution rose models attributed sulphur dioxide  
554 and sulphate in Milan to emission sources in the Po valley, in the Ligurian  
555 coast and Ligurian sea. Steady high levels of ammonia have been observed  
556 throughout the campaign, originated mostly by agricultural emissions within  
557 the whole Po valley. A distinct pattern was observed for hydrochloric acid:  
558 several potential sources were investigated and results hints to evaporation  
559 of a chlorinated compound, although further studies are needed to provide a

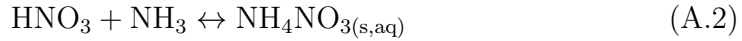
560 clear answer.

561 The atmospheric stability conditions enduring during the campaign al-  
562 lowed to investigate in details processing and ageing of several gas phase  
563 and aerosol pollutants. Overall variability has been checked by hierarchi-  
564 cal cluster analysis, with a distance matrix based on Pearson’s correlation  
565 coefficient (Bigi and Ghermandi, 2014) and grouping driven by a divisive  
566 algorithm (Kaufman and Rousseeuw, 1990). Results showed a strong cor-  
567 relation among most pollutants and a modest cluster structure, featured by  
568 two groups (Figure S14): the first group includes long range transported  
569 pollutants (e.g.  $\text{SO}_2$ ,  $\text{SO}_4^{2-}$ ) and compounds strongly correlated to radia-  
570 tion and temperature. The second group includes locally emitted and lo-  
571 cally formed pollutants, e.g. BC and  $\text{NO}_3^-$ . Implications of these results  
572 for local air quality policies are several: a large metropolitan area, although  
573 sited in a confined valley and under long-lasting atmospheric stability, can  
574 have air quality significantly affected by long-range transported pollutants.  
575 Moreover concentration variability of locally emitted pollutants in this same  
576 metropolitan area relies on the variability of overall emissions within the val-  
577 ley, therefore more attention needs to be paid to wide emissions, e.g. organic  
578 aerosol and ammonia. Conventional air quality policies aim to decrease con-  
579 centration of regulatory pollutants (e.g.  $\text{NO}_2$ ): we showed how their outcome  
580 controls the variation of less frequently monitored pollutants (e.g. HONO),  
581 whose influence on local air quality and climate is large and neglected by  
582 policymakers. Po valley plume stretches towards several European regions

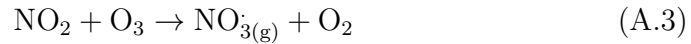
583 surrounding Italy on the East and South (Finardi et al., 2014), including  
 584 large parts of the Mediterranean sea, contributing to acidification and eu-  
 585 trophication (Jalkanen et al., 2000; Im et al., 2013). Study outlooks include  
 586 a source apportionment analysis and deeper investigation of carbonaceous  
 587 aerosol and secondary organic formation events.

## 588 **Appendix A. Nitrate formation pathways**

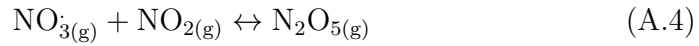
589 Formation of nitrate through homogeneous reaction pathway



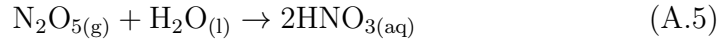
590 Formation of nitrate through heterogeneous reaction pathway with night-  
 591 time formation of nitrate radical  $\text{NO}_3\cdot$ , its reaction to dinitrogen pentoxide  
 592  $\text{N}_2\text{O}_5$ , the hydrolysis of  $\text{N}_2\text{O}_5$  on surfaces releasing  $\text{HNO}_{3(\text{aq})}$  which is finally  
 593 hydrolysed to nitrate, similarly to the reaction A.2.



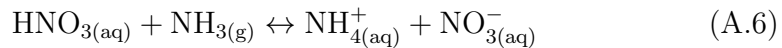
594



595



596



597 **Appendix B. Calculation of equilibrium constants for ammonium**  
 598 **nitrate**

599  $K_p$  and  $K_p^*$  are the dissociation constants for solid phase and aqueous  
 600 ammonium nitrate respectively, estimated according to Mozurkewich (1993).  
 601  $K_{AN}$  is the equilibrium constant for reaction A.2, estimated according to  
 602 Seinfeld and Pandis (2006) and Poulain et al. (2011).

603 Deliquescence relative humidity for ammonium nitrate (Seinfeld and Pan-  
 604 dis, 2006):

$$\ln(\text{DRH}) = \frac{723.7}{T} + 1.6954 \quad (\text{B.1})$$

605 Dissociation constant  $K_p$  for solid ammonium nitrate formed through  
 606 reaction A.2 (Mozurkewich, 1993):

$$\ln(K_p) = 118.87 - \frac{24084}{T} - 6.025 \ln(T) \quad (\text{B.2})$$

607 Dissociation constant  $K_p^*$  for aqueous ammonium nitrate formed through  
 608 reaction A.2 (Mozurkewich, 1993):

$$K_p^* = (P_1 - P_2(1 - a_w) + P_3(1 - a_w)^2) \cdot (1 - a_w)^{1.75} \cdot K_p \quad (\text{B.3})$$

609 with

$$\ln(P_1) = -135.94 + \frac{8763}{T} + 19.12 \ln(T) \quad (\text{B.4})$$

610

$$\ln(P_2) = -122.65 + \frac{9969}{T} + 16.22 \ln(T) \quad (\text{B.5})$$

611

$$\ln(P_1) = -182.61 + \frac{13875}{T} + 24.46 \ln(T) \quad (\text{B.6})$$

612

and water activity  $a_w$  approximated by RH expressed in the range 0–1.

613

Equilibrium constant  $K_{AN}$  of ammonium nitrate at RH above that of deli-

614

quescence ammonium nitrate, in ppb<sup>2</sup> from Poulain et al. (2011).

$$K_{AN} = k(298) \exp \left\{ a \left( \frac{298}{T} - 1 \right) + b \left[ 1 + \ln \left( \frac{298}{T} \right) - \frac{298}{T} \right] \right\} \cdot 10^{-18} \quad (\text{B.7})$$

615

with  $k(298) = 3.35 \cdot 10^{-16} \text{ atm}^{-2}$ ,  $a = 75.11$ ,  $b = -13.5$

616

**Acknowledgements** Thanks to Luca Lombroso for the description of the

617

synoptic meteorological conditions.

618

Acker, K., Mller, D., Auel, R., Wieprecht, W., and Kala, D.: Concentra-

619

tions of nitrous acid, nitric acid, nitrite and nitrate in the gas and aerosol

620

phase at a site in the emission zone during ESCOMPTE 2001 experiment,

621

Atmospheric Research, 74, 507 – 524, doi:10.1016/j.atmosres.2004.04.009,

622

2005.

623

AERA: OGC-WMS Server <http://geomap.reteunitaria.piemonte.it/ws/aera/rp->

624

01/aerawms/wms\_aera\_emissioni\_tot?, last access: 2015-01-07, 2015.

625

Alexander, B., Hastings, M. G., Allman, D. J., Dachs, J., Thornton, J. A.,

626

and Kunasek, S. A.: Quantifying atmospheric nitrate formation pathways

627

based on a global model of the oxygen isotopic composition ( $\Delta^{17}\text{O}$ ) of



628 atmospheric nitrate, *Atmospheric Chemistry and Physics*, 9, 5043–5056,  
629 doi:10.5194/acp-9-5043-2009, 2009.

630 Alicke, B., Platt, U., and Stutz, J.: Impact of nitrous acid photolysis on the  
631 total hydroxyl radical budget during the Limitation of Oxidant Produc-  
632 tion/Pianura Padana Produzione di Ozono study in Milan, *Journal of Geo-*  
633 *physical Research: Atmospheres*, 107, 8196, doi:10.1029/2000JD000075,  
634 2002.

635 Bae, M.-S., Schauer, J. J., DeMinter, J. T., Turner, J. R., Smith, D., and  
636 Cary, R. A.: Validation of a semi-continuous instrument for elemental  
637 carbon and organic carbon using a thermal-optical method, *Atmospheric*  
638 *Environment*, 38, 2885–2893, doi:10.1016/j.atmosenv.2004.02.027, 2004.

639 Baltensperger, U., Streit, N., Weingartner, E., Nyeki, S., Prévôt, A. S. H.,  
640 Van Dingenen, R., Virkkula, A., Putaud, J.-P., Even, A., ten Brink, H.,  
641 Blatter, A., Neftel, A., and Gägeler, H. W.: Urban and rural aerosol  
642 characterization of summer smog events during the PIPAPO field cam-  
643 paign in Milan, Italy, *Journal of Geophysical Research*, D107, 8193, doi:  
644 10.1029/2001JD001292, 2002.

645 Bari, A., Ferraro, V., Wilson, L. R., Luttinger, D., and Husain, L.: Mea-  
646 surements of gaseous HONO, HNO<sub>3</sub>, SO<sub>2</sub>, HCl, NH<sub>3</sub>, particulate sulfate  
647 and PM<sub>2.5</sub> in New York, NY, *Atmospheric Environment*, 37, 2825–2835,  
648 doi:10.1016/S1352-2310(03)00199-7, 2003.

- 649 Bernardoni, V., Vecchi, R., Valli, G., Piazzalunga, A., and Fermo,  
650 P.: PM10 source apportionment in Milan (Italy) using time-resolved  
651 data, *Science of The Total Environment*, 409, 4788 – 4795, doi:  
652 10.1016/j.scitotenv.2011.07.048, 2011.
- 653 Bigi, A. and Ghermandi, G.: Long-term trend and variability of atmospheric  
654 PM<sub>10</sub> concentration in the Po Valley, *Atmospheric Chemistry and Physics*,  
655 14, 4895–4907, doi:10.5194/acp-14-4895-2014, 2014.
- 656 Bigi, A. and Ghermandi, G.: Trends and variability of atmospheric PM<sub>2.5</sub>  
657 and PM<sub>10–2.5</sub> concentration in the Po Valley, Italy, *Atmospheric Chemistry*  
658 *and Physics Discussions*, under review.
- 659 Bigi, A., Ghermandi, G., and Harrison, R. M.: Analysis of the air pollution  
660 climate at a background site in the Po valley, *Journal of Environmental*  
661 *Monitoring*, 14, 552–563, doi:10.1039/c1em10728c, 2012.
- 662 Cabada, J., Pandis, S., Subramanian, R., Robinson, A., Polidori, A., and  
663 Turpin, B.: Estimating the Secondary Organic Aerosol Contribution to  
664 PM<sub>2.5</sub> Using the EC Tracer Method, *Aerosol Science and Technology*, 38,  
665 140–155, doi:10.1080/02786820390229084, 2004.
- 666 Carslaw, D. and Ropkins, K.: openair – an R package for air quality data  
667 analysis, *Environmental Modelling & Software*, 27–28, 52–61, 2012.
- 668 Cavalli, F., Viana, M., Yttri, K. E., Genberg, J., and Putaud, J.-P.: Toward  
669 a standardised thermal-optical protocol for measuring atmospheric organic

670 and elemental carbon: the EUSAAR protocol, *Atmospheric Measurement*  
 671 *Techniques*, 3, 79–89, doi:10.5194/amt-3-79-2010, 2010.

672 Cleveland, W. S., Graedel, T. E., Kleiner, B., and Warner, J. L.: Sunday and  
 673 Workday Variations in Photochemical Air Pollutants in New Jersey and  
 674 New York, *Science*, 186, 1037–1038, doi:10.1126/science.186.4168.1037,  
 675 1974.

676 Curci, G., Ferrero, L., Tuccella, P., Barnaba, F., Angelini, F., Bolzacchini,  
 677 E., Carbone, C., Denier van der Gon, H. A. C., Facchini, M. C., Gobbi,  
 678 G. P., Kuenen, J. P. P., Landi, T. C., Perrino, C., Perrone, M. G., San-  
 679 giorgi, G., and Stocchi, P.: How much is particulate matter near the ground  
 680 influenced by upper-level processes within and above the PBL? A summer-  
 681 time case study in Milan (Italy) evidences the distinctive role of nitrate,  
 682 *Atmospheric Chemistry and Physics*, 15, 2629–2649, doi:10.5194/acp-15-  
 683 2629-2015, 2015.

684 D’Alessandro, A., Lucarelli, F., Mand, P., Marcazzan, G., Nava, S., Prati, P.,  
 685 Valli, G., Vecchi, R., and Zucchiatti, A.: Hourly elemental composition and  
 686 sources identification of fine and coarse PM10 particulate matter in four  
 687 Italian towns, *Journal of Aerosol Science*, 34, 243–259, doi:10.1016/S0021-  
 688 8502(02)00172-6, 2003.

689 D’Alessandro, A., Lucarelli, F., Marcazzan, G., Nava, S., Prati, P., Valli,  
 690 G., Vecchi, R., and Zucchiatti, A.: A summertime investigation on urban

691 PM fine and coarse fractions using hourly elemental concentration data  
 692 series, *Nuovo Cimento della Societa Italiana di Fisica C*, 27, 17–28, doi:  
 693 10.1393/ncc/i2003-10015-7, 2004.

694 Draxler, R. and Rolph, G.: HYSPLIT (HYbrid Single-Particle Lagrangian  
 695 Integrated Trajectory), Model access via NOAA ARL READY Website  
 696 (<http://www.arl.noaa.gov/HYSPLIT.php>), 2013.

697 Eldering, A., Solomon, P. A., Salmon, L. G., Fall, T., and Cass, G. R.:  
 698 Hydrochloric acid: A regional perspective on concentrations and formation  
 699 in the atmosphere of Southern California, *Atmospheric Environment. Part*  
 700 *A. General Topics*, 25, 2091 – 2102, doi:10.1016/0960-1686(91)90086-M,  
 701 1991.

702 Febo, A., Perrino, C., and Allegrini, I.: Measurement of nitrous acid in  
 703 Milan, Italy, by DOAS and diffusion denuders, *Atmospheric Environment*,  
 704 30, 3599–3609, doi:10.1016/1352-2310(96)00069-6, 1996.

705 Finardi, S., Silibello, C., Dallura, A., and Radice, P.: Analysis  
 706 of pollutants exchange between the Po Valley and the surround-  
 707 ing European region, *Urban Climate*, 10, Part 4, 682 – 702, doi:  
 708 <http://dx.doi.org/10.1016/j.uclim.2014.02.002>, 2014.

709 Finlayson-Pitts, B. J. and Pitts, J. N.: *Chemistry of the upper and lower*  
 710 *atmosphere*, Academic Press, San Diego, USA, 2000.

711 Fleming, Z. L., Monks, P. S., and Manning, A. J.: Review: Un-  
 712 tangling the influence of air-mass history in interpreting observed at-  
 713 mospheric composition, *Atmospheric Research*, 104105, 1 – 39, doi:  
 714 10.1016/j.atmosres.2011.09.009, 2012.

715 Fountoukis, C. and Nenes, A.: ISORROPIA II: a computationally efficient  
 716 thermodynamic equilibrium model for  $\text{K}^+ - \text{Ca}^{2+} - \text{Mg}^{2+} - \text{NH}_4^+ - \text{Na}^+ - \text{SO}_4^{2-} -$   
 717  $\text{NO}_3^- - \text{Cl}^- - \text{H}_2\text{O}$  aerosols, *Atmospheric Chemistry and Physics*, 7, 4639–  
 718 4659, doi:10.5194/acp-7-4639-2007, 2007.

719 Gutzwiller, L., Arens, F., Baltensperger, U., Gggeler, H. W., and Ammann,  
 720 M.: Significance of Semivolatile Diesel Exhaust Organics for Secondary  
 721 HONO Formation, *Environmental Science & Technology*, 36, 677–682, doi:  
 722 10.1021/es015673b, 2002.

723 Han, Y., , Holsen, T., Hopke, P., and Yi, S.: Comparison between Back-  
 724 Trajectory Based Modeling and Lagrangian Backward Dispersion Mod-  
 725 eling for Locating Sources of Reactive Gaseous Mercury, *Environmental*  
 726 *Science & Technology*, 39, 1715–1723, doi:10.1021/es0498540, 2005.

727 Henschel, S., Querol, X., Atkinson, R., Pandolfi, M., Zeka, A., Tertre,  
 728 A. L., Analitis, A., Katsouyanni, K., Chanel, O., Pascal, M., Bouland,  
 729 C., Haluza, D., Medina, S., and Goodman, P. G.: Ambient air  $\text{SO}_2$  pat-  
 730 terns in 6 European cities, *Atmospheric Environment*, 79, 236–247, doi:  
 731 10.1016/j.atmosenv.2013.06.008, 2013.

732 Im, U., Christodoulaki, S., Violaki, K., Zampas, P., Kocak, M., Daskalakis,  
733 N., Mihalopoulos, N., and Kanakidou, M.: Atmospheric deposition of  
734 nitrogen and sulfur over southern Europe with focus on the Mediter-  
735 ranean and the Black Sea, *Atmospheric Environment*, 81, 660–670, doi:  
736 10.1016/j.atmosenv.2013.09.048, 2013.

737 INEMAR: [www.inemar.eu](http://www.inemar.eu), last access: 2015-01-07, 2015.

738 Jalkanen, L., Mkinen, A., Hsnen, E., and Juhanoja, J.: The effect of large  
739 anthropogenic particulate emissions on atmospheric aerosols, deposition  
740 and bioindicators in the eastern Gulf of Finland region, *Science of the Total*  
741 *Environment*, 262, 123–136, doi:10.1016/S0048-9697(00)00602-1, 2000.

742 Jarvis, A., Reuter, H. I., Nelson, A., and Guevara, E.: Hole-filled seamless  
743 SRTM data V4, Tech. rep., International Centre for Tropical Agriculture  
744 (CIAT), URL <http://srtm.csi.cgiar.org>, 2008.

745 Jiménez, P., Parra, R., Gassó, S., and Baldasano, J. M.: Modeling the  
746 ozone weekend effect in very complex terrains: a case study in the North-  
747 eastern Iberian Peninsula, *Atmospheric Environment*, 39, 429 – 444, doi:  
748 <http://dx.doi.org/10.1016/j.atmosenv.2004.09.065>, 2005.

749 Jung, J., Kim, Y. J., Lee, K. Y., Kawamura, K., Hu, M., and Kondo, Y.:  
750 The effects of accumulated refractory particles and the peak inert mode  
751 temperature on semi-continuous organic carbon and elemental carbon mea-

752 surements during the CAREBeijing 2006 campaign, *Atmospheric Environ-*  
 753 *ment*, 45, 7192 – 7200, doi:10.1016/j.atmosenv.2011.09.003, 2011.

754 Kalberer, M., Ammann, M., Arens, F., Gggeler, H. W., and Baltensperger,  
 755 U.: Heterogeneous formation of nitrous acid (HONO) on soot aerosol par-  
 756 ticles, *Journal of Geophysical Research: Atmospheres*, 104, 13 825–13 832,  
 757 doi:10.1029/1999JD900141, 1999.

758 Kaneyasu, N., Yoshikado, H., Mizuno, T., Sakamoto, K., and Soufuku, M.:  
 759 Chemical forms and sources of extremely high nitrate and chloride in winter  
 760 aerosol pollution in the Kanto Plain of Japan, *Atmospheric Environment*,  
 761 33, 1745 – 1756, doi:10.1016/S1352-2310(98)00396-3, 1999.

762 Kaufman, L. and Rousseeuw, P. J.: *Finding groups in data : an introduction*  
 763 *to cluster analysis*, Wiley, New York, 1990.

764 Kleffmann, J.: Daytime Sources of Nitrous Acid (HONO) in the  
 765 Atmospheric Boundary Layer, *ChemPhysChem*, 8, 1137–1144, doi:  
 766 10.1002/cphc.200700016, 2007.

767 Kleffmann, J., Lrzer, J., Wiesen, P., Kern, C., Trick, S., Volkamer, R., Ro-  
 768 denas, M., and Wirtz, K.: Intercomparison of the DOAS and LOPAP  
 769 techniques for the detection of nitrous acid (HONO), *Atmospheric Envi-*  
 770 *ronment*, 40, 3640 – 3652, doi:10.1016/j.atmosenv.2006.03.027, 2006.

771 Kurtenbach, R., Becker, K., Gomes, J., Kleffmann, J., Lrzer, J., Spittler,  
 772 M., Wiesen, P., Ackermann, R., Geyer, A., and Platt, U.: Investiga-

773 tions of emissions and heterogeneous formation of HONO in a road traffic  
 774 tunnel, *Atmospheric Environment*, 35, 3385 – 3394, doi:10.1016/S1352-  
 775 2310(01)00138-8, 2001.

776 Lammel, G. and Cape, J. N.: Nitrous acid and nitrite in the atmosphere,  
 777 *Chem. Soc. Rev.*, 25, 361–369, doi:10.1039/CS9962500361, 1996.

778 Lightowers, P. and Cape, J.: Sources and fate of atmospheric HCl in the  
 779 U.K. and Western Europe, *Atmospheric Environment* (1967), 22, 7 – 15,  
 780 doi:10.1016/0004-6981(88)90294-6, 1988.

781 Lonati, G., Ozgen, S., and Giugliano, M.: Primary and secondary carbona-  
 782 ceous species in PM<sub>2.5</sub> samples in Milan (Italy), *Atmospheric Environ-*  
 783 *ment*, 41, 4599 – 4610, doi:10.1016/j.atmosenv.2007.03.046, 2007.

784 Marcazzan, G., Caprioli, E., Valli, G., and Vecchi, R.: Temporal variation of  
 785 <sup>212</sup>Pb concentration in outdoor air of Milan and a comparison with <sup>214</sup>Pb,  
 786 *Journal of Environmental Radioactivity*, 65, 77–90, doi:10.1016/S0265-  
 787 931X(02)00089-9, 2003.

788 Markovic, M. Z., VandenBoer, T. C., and Murphy, J. G.: Characteriza-  
 789 tion and optimization of an online system for the simultaneous mea-  
 790 surement of atmospheric water-soluble constituents in the gas and par-  
 791 ticle phases, *Journal of Environmental Monitoring*, 14, 1872–1884, doi:  
 792 10.1039/C2EM00004K, 2012.



- 793 Michalski, G., Scott, Z., Kabling, M., and Thiemens, M. H.: First measure-  
794 ments and modeling of  $\Delta^{17}\text{O}$  in atmospheric nitrate, *Geophysical Research*  
795 *Letters*, 30, doi:10.1029/2003GL017015, 2003.
- 796 Michoud, V., Colomb, A., Borbon, A., Miet, K., Beekmann, M., Camre-  
797 don, M., Aumont, B., Perrier, S., Zapf, P., Siour, G., Ait-Helal, W., Afif,  
798 C., Kukui, A., Furger, M., Dupont, J. C., Haeffelin, M., and Doussin,  
799 J. F.: Study of the unknown HONO daytime source at a European sub-  
800 urban site during the MEGAPOLI summer and winter field campaigns,  
801 *Atmospheric Chemistry and Physics*, 14, 2805–2822, doi:10.5194/acp-14-  
802 2805-2014, 2014.
- 803 Mozurkewich, M.: The dissociation constant of ammonium nitrate and  
804 its dependence on temperature, relative humidity and particle size, *At-*  
805 *mospheric Environment. Part A. General Topics*, 27, 261 – 270, doi:  
806 [http://dx.doi.org/10.1016/0960-1686\(93\)90356-4](http://dx.doi.org/10.1016/0960-1686(93)90356-4), 1993.
- 807 Neftel, A., Spirig, C., Prévôt, A. S. H., Furger, M., Stutz, J., Vogel, B., and  
808 Hjorth, J.: Sensitivity of photooxidant production in the Milan Basin: An  
809 overview of results from a EUROTRAC-2 Limitation of Oxidant Produc-  
810 tion field experiment, *Journal of Geophysical Research: Atmospheres*, 107,  
811 8188, doi:10.1029/2001JD001263, 2002.
- 812 Penkett, S., Jones, B., Brich, K., and Eggleton, A.: The importance of  
813 atmospheric ozone and hydrogen peroxide in oxidising sulphur dioxide in

cloud and rainwater, *Atmospheric Environment* (1967), 13, 123 – 137, doi:  
10.1016/0004-6981(79)90251-8, 1979.

Perrone, M., Larsen, B., Ferrero, L., Sangiorgi, G., Gennaro, G. D., Udisti,  
R., Zangrando, R., Gambaro, A., and Bolzacchini, E.: Sources of high  
PM<sub>2.5</sub> concentrations in Milan, Northern Italy: Molecular marker data  
and CMB modelling, *Science of The Total Environment*, 414, 343 – 355,  
doi:10.1016/j.scitotenv.2011.11.026, 2012.

Petzold, A., Kramer, H., and Schönlinner, M.: Continuous measurement  
of atmospheric black carbon using a multi-angle absorption photometer,  
*Environmental Science and Pollution Research*, 4, 78–82, 2002.

Pollack, I., Ryerson, T., Trainer, M., Parrish, D., Andrews, A., Atlas, E.,  
Blake, D., Brown, S., Commane, R., Daube, B., De Gouw, J., Dub, W.,  
Flynn, J., Frost, G., Gilman, J., Grossberg, N., Holloway, J., Kofler, J.,  
Kort, E., Kuster, W., Lang, P., Lefer, B., Lueb, R., Neuman, J., Nowak,  
J., Novelli, P., Peischl, J., Perring, A., Roberts, J., Santoni, G., Schwarz,  
J., Spackman, J., Wagner, N., Warneke, C., Washenfelder, R., Wofsy,  
S., and Xiang, B.: Airborne and ground-based observations of a weekend  
effect in ozone, precursors, and oxidation products in the California South  
Coast Air Basin, *Journal of Geophysical Research: Atmospheres*, 117, doi:  
10.1029/2011JD016772, 2012.

Poulain, L., Spindler, G., Birmili, W., Plass-Dülmer, C., Wiedensohler, A.,  
and Herrmann, H.: Seasonal and diurnal variations of particulate nitrate

and organic matter at the IfT research station Melpitz, Atmospheric Chem-  
 istry and Physics, 11, 12 579–12 599, doi:10.5194/acp-11-12579-2011, 2011.

Putaud, J.-P., Van Dingenen, R., and Raes, F.: Submicron aerosol mass bal-  
 ance at urban and semirural sites in the Milan area (Italy), Journal of Geo-  
 physical Research: Atmospheres, 107, 8198, doi:10.1029/2000JD000111,  
 2002.

Putaud, J.-P., Van Dingenen, R., Alastuey, A., Bauer, H., Birmili, W., Cyrys,  
 J., Flentje, H., Fuzzi, S., Gehrig, R., Hansson, H. C., Harrison, R. M., Her-  
 rmann, H., Hittenberger, R., Hglin, C., Jones, A. M., Kasper-Giebl, A.,  
 Kiss, G., Kousa, A., Kuhlbusch, T. A. J., Lschau, G., Maenhaut, W.,  
 Molnar, A., Moreno, T., Pekkanen, J., Perrino, C., Pitz, M., Puxbaum,  
 H., Querol, X., Rodriguez, S., Salma, I., Schwarz, J., Smolik, J., Schnei-  
 der, J., Spindler, G., ten Brink, H., Tursic, J., Viana, M., Wiedensohler,  
 A., and Raes, F.: A European aerosol phenomenology - 3: Physical and  
 chemical characteristics of particulate matter from 60 rural, urban, and  
 kerbside sites across Europe, Atmospheric Environment, 44, 1308 – 1320,  
 doi:10.1016/j.atmosenv.2009.12.011, 2010.

R Core Team: R: A Language and Environment for Statistical Computing,  
 R Foundation for Statistical Computing, Vienna, Austria, 2013.

Ravishankara, A. R.: Heterogeneous and Multiphase Chemistry in the Tropo-  
 sphere, Science, 276, 1058–1065, doi:10.1126/science.276.5315.1058, 1997.

- 857 Richards, L., Anderson, J., Blumenthal, D., Brandt, A., McDonald, J., Wa-  
858 ters, N., Macias, E., and Bhardwaja, P.: Plumes and Visibility Measure-  
859 ments and Model Components The chemistry, aerosol physics, and optical  
860 properties of a western coal-fired power plant plume, *Atmospheric Environ-*  
861 *ment*, 15, 2111 – 2134, doi:[http://dx.doi.org/10.1016/0004-6981\(81\)90245-](http://dx.doi.org/10.1016/0004-6981(81)90245-6)  
862 6, 1981.
- 863 Scheifinger, H. and Kaiser, A.: Validation of trajectory statis-  
864 tical methods, *Atmospheric Environment*, 41, 8846–8856, doi:  
865 [10.1016/j.atmosenv.2007.08.034](http://dx.doi.org/10.1016/j.atmosenv.2007.08.034), 2007.
- 866 Seinfeld, J. H. and Pandis, S. N.: *Atmospheric Chemistry and Physics*, Wiley,  
867 2nd edn., 2006.
- 868 Spindler, G., Hesper, J., Brüggemann, E., Dubois, R., Müller, T., and Her-  
869 rmann, H.: Wet annular denuder measurements of nitrous acid: laboratory  
870 study of the artefact reaction of NO<sub>2</sub> with S(IV) in aqueous solution and  
871 comparison with field measurements, *Atmospheric Environment*, 37, 2643  
872 – 2662, doi:[http://dx.doi.org/10.1016/S1352-2310\(03\)00209-7](http://dx.doi.org/10.1016/S1352-2310(03)00209-7), 2003.
- 873 Stutz, J., Alicke, B., and Neftel, A.: Nitrous acid formation in the urban  
874 atmosphere: Gradient measurements of NO<sub>2</sub> and HONO over grass in  
875 Milan, Italy, *Journal of Geophysical Research: Atmospheres*, 107, doi:  
876 [10.1029/2001JD000390](http://dx.doi.org/10.1029/2001JD000390), 2002.
- 877 Tonse, S., Brown, N., Harley, R., and Jin, L.: A process-analysis based study

878 of the ozone weekend effect, *Atmospheric Environment*, 42, 7728–7736, doi:  
 879 10.1016/j.atmosenv.2008.05.061, 2008.

880 Uria-Tellaetxe, I. and Carslaw, D. C.: Conditional bivariate probability func-  
 881 tion for source identification, *Environmental Modelling & Software*, 59, 1  
 882 – 9, doi:<http://dx.doi.org/10.1016/j.envsoft.2014.05.002>, 2014.

883 Vecchi, R. and Valli, G.: Ozone assessment in the southern part of the Alps,  
 884 *Atmospheric Environment*, 33, 97–109, doi:10.1016/S1352-2310(98)00133-  
 885 2, 1999.

886 Vecchi, R., Valli, G., Fermo, P., D’Alessandro, A., Piazzalunga,  
 887 A., and Bernardoni, V.: Organic and inorganic sampling arte-  
 888 facts assessment, *Atmospheric Environment*, 43, 1713 – 1720, doi:  
 889 10.1016/j.atmosenv.2008.12.016, 2009.

890 Vecchi, R., Valli, G., Bernardoni, V., Paganelli, C., and Piazzalunga, A.:  
 891 Insights on BC determination on quartz-fibre and PTFE filters: results of  
 892 two field experiments in Milan (Italy), in: *Proceedings of the European*  
 893 *Aerosol Conference 2012*, edited by Alados-Arboledas, L. and Olmo Reyes,  
 894 F. J., AWG08S1P17, European Aerosol Assembly, Granada, Spain, 2012.

895 Wang, Y., Hu, B., Ji, D., Liu, Z., Tang, G., Xin, J., Zhang, H., Song, T.,  
 896 Wang, L., Gao, W., Wang, X., and Wang, Y.: Ozone weekend effects in the  
 897 Beijing-Tianjin-Hebei metropolitan area, China, *Atmospheric Chemistry*  
 898 *and Physics*, 14, 2419–2429, doi:10.5194/acp-14-2419-2014, 2014.

- 899 Wood, S.: Generalized Additive Models: an introduction with R, Chapman  
900 & Hall/CRC, Boca Raton, USA, 2006.
- 901 World Health Organization: Air quality guidelines. Global update 2005. Par-  
902 ticulate matter, ozone, nitrogen dioxide and sulfur dioxide, World Health  
903 Organization, Regional office for Europe, Copenhagen, Denmark, 2006.
- 904 Zhang, J. and Trivikrama Rao, S.: The Role of Vertical Mixing  
905 in the Temporal Evolution of Ground-Level Ozone Concentrations,  
906 Journal of Applied Meteorology, 38, 1674–1691, doi:10.1175/1520-  
907 0450(1999)038<1674:TROVMI>2.0.CO;2, 1999.
- 908 Ziemba, L. D., Dibb, J. E., Griffin, R. J., Anderson, C. H., Whitlow, S. I.,  
909 Lefer, B. L., Rappenglek, B., and Flynn, J.: Heterogeneous conversion  
910 of nitric acid to nitrous acid on the surface of primary organic aerosol in  
911 an urban atmosphere, Atmospheric Environment, 44, 4081 – 4089, doi:  
912 10.1016/j.atmosenv.2008.12.024, 2010.

Table B.1: Statistical values of gas, particles and meteorological parameters during the whole campaign. Note: for global radiation the range of maximum diurnal is indicated; for precipitation the total rainfall and the maxium intensity are indicated.

Parameter	Mean $\pm \sigma$	Median
Nitric oxide (NO), ppb	4.58 $\pm$ 2.66	4.00
Nitrogen dioxide (NO <sub>2</sub> ), ppb	6.41 $\pm$ 6.46	4.18
Nitrogen oxides as NO <sub>2</sub> (NO <sub>x</sub> ), ppb	10.99 $\pm$ 8.10	8.00
Ozone (O <sub>3</sub> ), ppb	41.73 $\pm$ 19.73	41.10
Organic carbon (OC), $\mu\text{g m}^{-3}$	6.16 $\pm$ 4.53	4.42
Elemental carbon (EC), $\mu\text{g m}^{-3}$	0.70 $\pm$ 0.61	0.62
Equivalent black carbon (BC <sub>E</sub> ), $\mu\text{g m}^{-3}$	1.59 $\pm$ 1.16	1.25
Hydrochloric acid (HCl), ppb	0.19 $\pm$ 0.20	0.12
Ammonia (NH <sub>3</sub> ), ppb	14.40 $\pm$ 5.25	13.18
Nitrous acid (HONO), ppb	0.55 $\pm$ 0.34	0.49
Nitric acid (HNO <sub>3</sub> ), ppb	0.71 $\pm$ 0.51	0.60
Sulphur dioxide (SO <sub>2</sub> ), ppb	0.92 $\pm$ 0.50	0.79
Calcium ion (Ca <sup>2+</sup> ), $\mu\text{g m}^{-3}$	0.27 $\pm$ 0.21	0.20
Chloride ion (Cl <sup>-</sup> ), $\mu\text{g m}^{-3}$	0.10 $\pm$ 0.21	0.10
Potassium ion (K <sup>+</sup> ), $\mu\text{g m}^{-3}$	0.08 $\pm$ 0.18	0.10
Magnesium ion (Mg <sup>2+</sup> ), $\mu\text{g m}^{-3}$	0.04 $\pm$ 0.10	0.00
Sodium ion (Na <sup>+</sup> ), $\mu\text{g m}^{-3}$	0.67 $\pm$ 0.79	0.30
Ammonium ion (NH <sub>4</sub> <sup>+</sup> ), $\mu\text{g m}^{-3}$	5.63 $\pm$ 3.40	5.00
Nitrite ion (NO <sub>2</sub> <sup>-</sup> ), $\mu\text{g m}^{-3}$	1.01 $\pm$ 0.58	0.90
Nitrate ion (NO <sub>3</sub> <sup>-</sup> ), $\mu\text{g m}^{-3}$	2.72 $\pm$ 3.15	1.80
Sulphate ion (SO <sub>4</sub> <sup>2-</sup> ), $\mu\text{g m}^{-3}$	4.82 $\pm$ 2.22	4.60
Atmospheric pressure (p), hPa	996.6 $\pm$ 3.9	996.3
Atmospheric temperature (T), C	26.0 $\pm$ 4.5	25.8
Global radiation (GR), W m <sup>-2</sup>	396.20 – 909.67	
Precipitation (r), mm – mm h <sup>-1</sup>	134.8 – 29.4	
Radon (Rn), Bq m <sup>-3</sup>	6.1 $\pm$ 4.0	4.8
Relative humidity (RH), %	51.9 $\pm$ 16.0	50.4
Wind speed (W), m s <sup>-1</sup>	1.2 $\pm$ 0.9	1.1

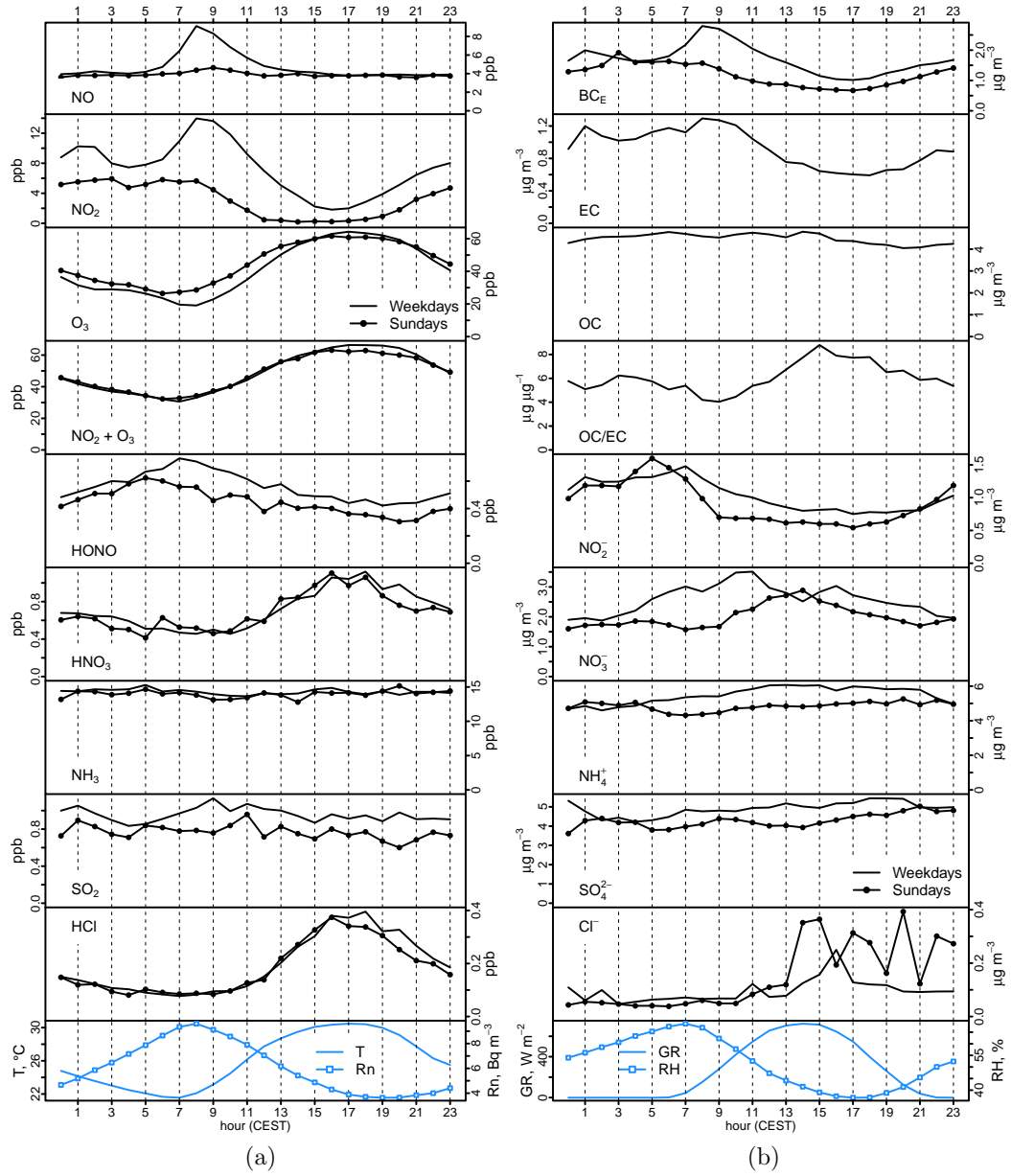


Figure B.1: Diurnal pattern for weekdays and Sundays for several gas phase (panel a) and particle phase (panel b) pollutants. Diurnal pattern of few meteorological variables and parameters are also included: temperature (T), Radon concentration (Rn), global radiation (GR) and relative humidity (RH).



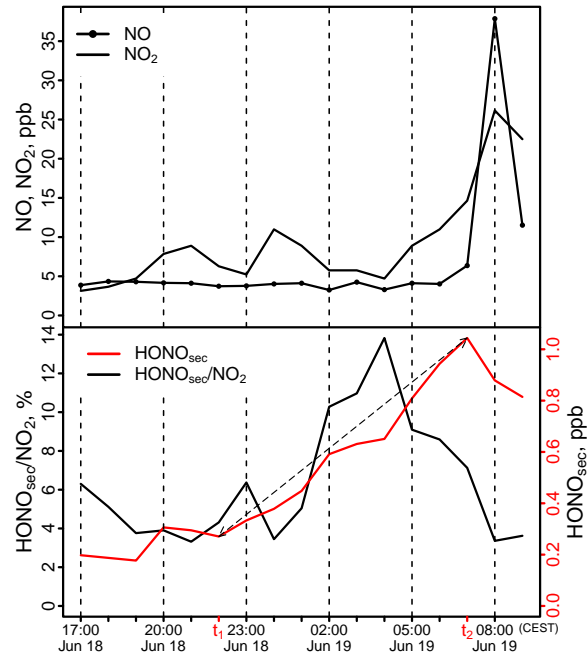


Figure B.2: Formation of  $\text{HONO}_{\text{sec}}$  during the night between June 18<sup>th</sup>–19<sup>th</sup> 2012. The arrows indicate the data used to calculate first-order formation rate.

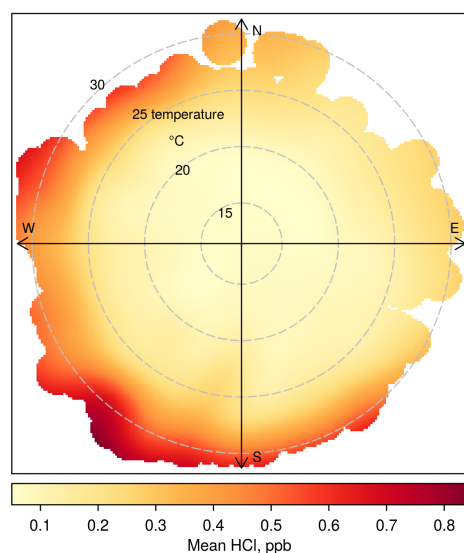


Figure B.3: Bivariate polar plots for hydrochloric acid with atmospheric temperature ( °C) as radial scale.

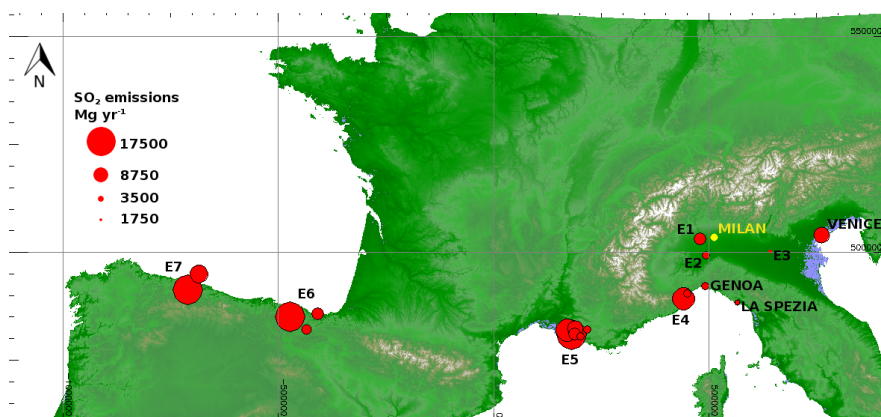


Figure B.4: Annual SO<sub>2</sub> emissions from point sources which potentially impacted on sulphur dioxide and sulphate ambient concentration in Milan in summer 2012 (DEM provided by Jarvis et al. (2008)).

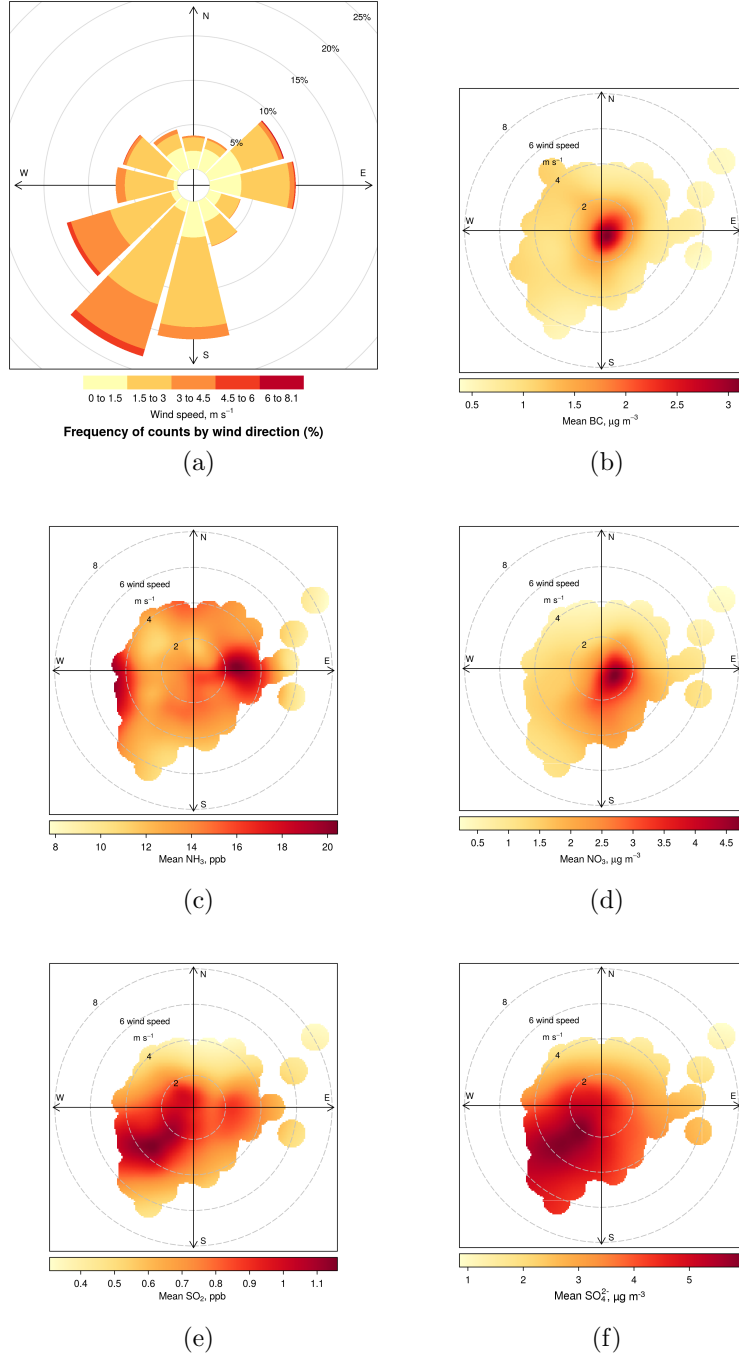


Figure B.5: Wind rose and bivariate polar plot of  $\text{BC}_E$ ,  $\text{NH}_3$ ,  $\text{NO}_3^-$ ,  $\text{SO}_2$  and  $\text{SO}_4^{2-}$ ; colour codes correspond to concentration for each direction; circles correspond to wind speed.

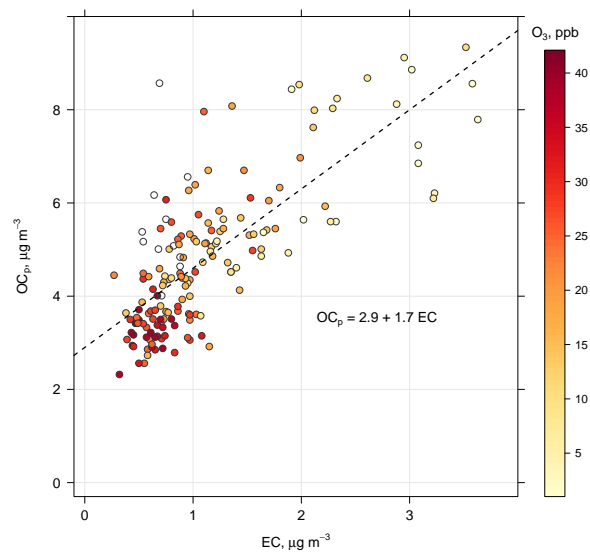


Figure B.6: Scatter plot of primary-dominated OC (OC<sub>p</sub>) vs EC data, colour-coded according to O<sub>3</sub> levels. Dashed line represents the linear regression model fit for the estimate of the OC<sub>p</sub>/EC ratio.

**Supplementary Material**

[Click here to download Supplementary Interactive Plot Data \(CSV\): supplementary\\_material\\_rev.pdf](#)